

Tu Verg 10

Surface-wave Dispersion Inversion versus SH-wave Refraction Tomography in Saturated and Poorly Dispersive Quick Clays

S. Pasquet* (UPMC - UMR 7619 Metis), G. Sauvin (ICG/UiO/NORSAR), M.R. Andriamboavonjy (SGDM/ESPA), L. Bodet (UPMC - UMR 7619 Metis), I. Lecomte (ICG/NORSAR/UiO) & R. Guérin (UPMC - UMR 7619 Metis)

SUMMARY

A seismic survey involving two distinct acquisition setups, with vertical and horizontal component geophones, has been carried out along the same line on a site presenting a simple vertical structure (peat, quick clays and bedrock) and no strong lateral variations. SH-wave refraction tomography and Rayleigh-wave dispersion inversion provided the same shear-wave velocity gradient in the quick clays. SH-wave tomography failed to correctly depict the peat layer and to reach the bedrock. A collection of Rayleigh-wave dispersion images were extracted along the line using windowing and stacking techniques. A thorough analysis of these images made it possible to give a complete description of the site velocity structure, illustrating the complementarity of both methods.

Introduction

Geophysical measurements were performed in an experimental site (Dragvoll, Norway) to characterise the physical properties of quick clays. Seismic methods have been proposed to focus on their mechanical properties through the combined study of pressure (P-) and shear (S-) wave velocities (V_p and V_s). While P-wave seismic methods can be considered well-established, measurements of V_s remain delicate because of well-known shear-wave generation and picking issues. As an alternative to SH-wave tomography, surface-wave methods are now classically suggested (e.g. Socco et al. 2010). Pseudo-2D V_s sections can be retrieved through specific processing techniques, using offset-moving windows and dispersion stacking to narrow down the lateral extent of dispersion measurements (e.g. Bergamo et al., 2012). Recent studies even tend to demonstrate that P-wave reflection, P-wave refraction and surface-wave dispersion data can be simultaneously acquired to infer the geometry, V_p and V_s of the investigated medium from a single seismic setup (Konstantaki et al. 2013).

Simultaneously retrieving 2D V_p and V_s sections with such optimised approach appears promising and attractive in terms of time and equipment costs, more particularly in the context of near-surface applications (at depth lower than 100 m). But refraction tomography and surface-wave dispersion inversion obviously involve distinct characteristics of the wavefield and different assumptions about the medium. The methods for instance provide results of different resolutions and investigation depths. This study tackles such issue through a systematic comparison of V_s models obtained from SH-wave refraction tomography and surface-wave dispersion inversion.

Context and site description

Quick clay landslides are a common hazard in formerly-glaciated coastal areas such as Norway, Sweden or Canada. Only small perturbations in stress conditions (e.g. human activity, erosion or heavy rainfall) can trigger a failure. Quick clay materials originate from highly porous clay deposited in marine environment during and/or following the last glacial age. After deglaciation, the isostatic rebound resulted in lowering the relative sea level, and led the former marine deposits to lie above the sea level. In such fresh-water environments, the salt which originally contributed to bond clay particles together can be leached from the clay material. When leaching of salt is sufficient, these clays can become highly sensitive or “quick” (Sauvin et al. 2013).

The presented survey was conducted in October 2012 in an experimental site located at about 2 km southeast of Trondheim, in the area of Dragvoll. The site is a flat square field of about 100 m per side, with a thin (less than 1 m) layer of peat at the surface. Below that superficial layer lie fully-saturated quick clays, filling a bowl-shaped basin formed by the eroded bedrock. In the southeast part of the site, the bedrock is almost outcropping, while it goes until 30 m down under the surface in the northwest part.

Acquisition methodology

The seismic survey consisted in a simultaneous P- and surface-wave acquisition followed by a SH-wave acquisition along the same line. The seismic profile was oriented northwest-southeast with a slight dip from southeast to northwest (around 3 %). A 72 channel Geometrics seismic recorder was used with 72 14 Hz vertical component geophones for the P-wave profile, and 72 14 Hz horizontal component geophones for the S-wave profile. A 1-m receiver spacing was used with one roll-along (shift of 24 receivers) to obtain a 95-m long profile. First shot location was one half receiver spacing away from first trace, and move up between shots was one receiver interval. 146 shots were recorded along the profile for a total number of 10512 active traces. The P-wave source consisted in an aluminium plate hit vertically by a 7 kg sledgehammer. The plate was hit 6 times at each position to increase signal-to-noise ratio. The SH-waves were produced with a manual source consisting of a heavy metal frame hit laterally by a 7 kg sledgehammer. The manual source was hit 8 times at each

position. For both P- and SH-wave acquisitions, the sampling rate was 1 ms and the recording time was 2 s (anticipating low propagation velocities).

Traveltime tomography

Collected data are of good quality with low noise level, and did not require specific processing other than basic trace normalisation. P- and SH-wave traveltimes could be identified and picked easily in the raw data from near to long offsets. Traveltime data were inverted with the refraction tomography software Rayfract (Schuster and Quintus-Bosz 1993; Sheehan et al. 2005) using a smooth gradient initial model. The inversion process was stopped when the global RMS error and the maximum single trace RMS error both reached a minimum value. With both P- and SH-wave traveltimes, 15 iterations were needed. The final 2D velocity models (Figure 1) were clipped below ray coverage of 100.

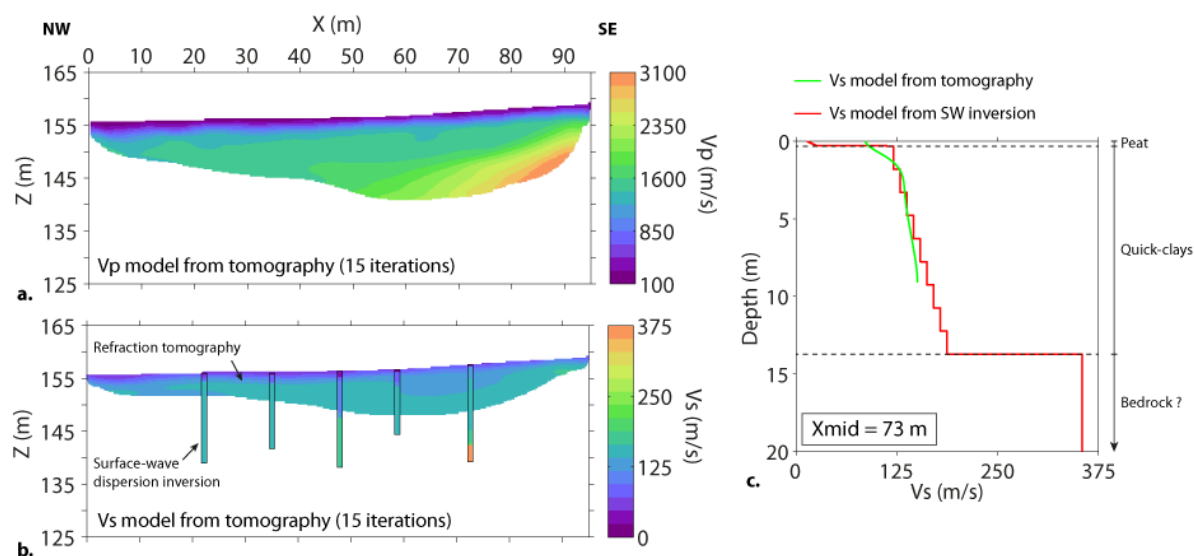


Figure 1 P-wave (a) and SH-wave (b) velocity models obtained after traveltime tomography. V_s models retrieved from surface-wave dispersion inversion are also superimposed on the V_s tomography model. (c) 1D velocity structures extracted at one surface-wave spread midpoint position (X_{mid}).

Both V_p (Figure 1a) and V_s (Figure 1b) models present a thin low velocity layer at the surface, followed by linearly increasing velocities. The V_p section presents a velocity increase in the southeastern end of the line, while the V_s model appears laterally homogeneous. The dipping structure suggested by V_p is in good agreement with *a priori* geological features, and most certainly corresponds to the bedrock. Due to the low velocity gradient in quick clays, SH-wave rays obviously fail to reach the bedrock.

Rayleigh-wave dispersion inversion

Our dense multifold acquisition setup allowed us to extract surface-wave dispersion images along the profile. The wavefield was transformed to the frequency-phase velocity ($p-\omega$) domain in which maxima should correspond to surface-wave propagation modes. Anticipating slight shallow lateral variations, we used a 41-trace extraction window (40 m). We stacked dispersion data extracted from 6 near-offset shots (3 direct and 3 reverse) in order to increase signal-to-noise ratio and check the validity of the 1D assumption. The moving window was shifted along the line to extract dispersion data at 5 evenly spaced spread mid-points (X_{mid}).

The stacking process clearly improved the quality of obtained dispersion images which still present a strong “effective character”. To facilitate mode identification, we relied on preliminary inversions and trial and error forward modelling based on *a priori* geological knowledge and results from refraction tomography. Such approach actually highlighted a “mode-jump” occurring around 20 Hz on each

dispersion image and confirmed the presence of overlapping modes. Such features were previously observed by Forbriger (2003a, 2003b) and O'Neill and Matsuoka (2005), and probably originate from the conjugate presence of a thin low velocity layer in surface (peat) and a velocity gradient down below (quick clays).

Assuming a 1D tabular medium below each extraction window, we performed 1D inversion of dispersion data at each X_{mid} . We used the Neighbourhood Algorithm (NA) implemented for near-surface applications by Wathelet et al. (2004), which performs a stochastic search of a pre-defined parameter space (namely V_p , V_s , density and thickness of each layer). We used a parameterisation with a stack of two layers (divided in 10 sub-layers following a linear increase of velocity with depth) overlaying the half-space. The half-space depth (HSD), of great importance since it depends on the poorly known depth of investigation of the method, was fixed to 50 % of the maximum observed wavelength as recommended by Bodet et al. (2009). The valid parameter ranges for sampling velocity models was 10 to 250 m/s for V_s in the two top layers and 10 to 500 m/s in the half-space. P-wave velocity being of weak constraint on surface-wave dispersion, only S-wave velocity profile can be interpreted. V_p however remains part of the actual parameter space and were generated in the range 10 to 3000 m/s. Density was set as uniform (1800 kg/m³). Dispersion data were inverted generating a total of 80400 models. Models matching the observed data within the error bars were selected to estimate an average velocity model at each position.

These average 1D V_s models were superimposed over the V_s tomography model (Figure 1b). Despite the use of a strict investigation depth criterion, recorded wavelengths made it possible to investigate deeper than tomography (down to 15-20 m against 5-10 m for tomography models). A thin layer (thickness varying between 0.3 and 0.6 m) with very low shear-wave velocity (around 50 m/s) is detected at the site surface. It can be associated with the saturated and unconsolidated peat layer. Underneath, the inversion leads to a linearly increasing velocity layer (from 125 to 225 m/s) which corresponds to quick-clays, and is in very good agreement with the tomography (see example on Figure 1c). The influence of the bedrock can be observed in the southeastern part of the profile with an increase of V_s , consistent with the V_p increase observed on the tomography model.

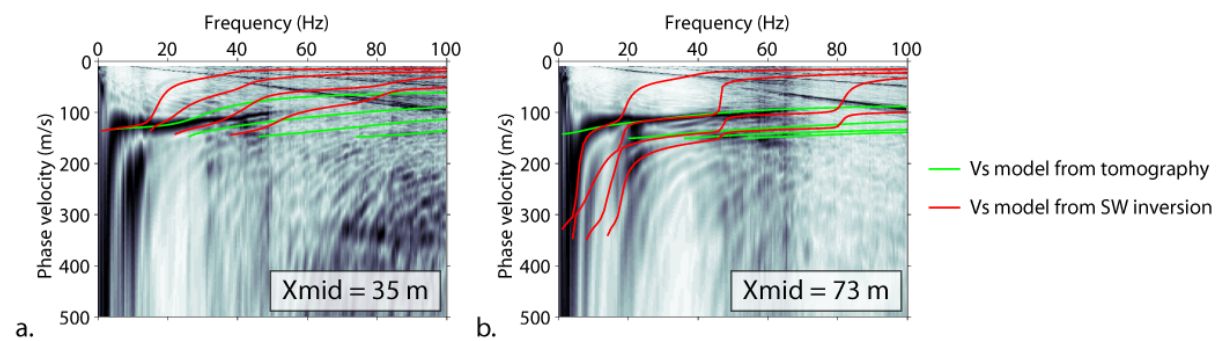


Figure 2 Stacked dispersion images at $X_{mid} = 35$ m (a) and $X_{mid} = 73$ m (b) with a 41-trace moving window (40 m). Dispersion curves calculated from both surface-wave dispersion inversion and tomography models are drawn respectively in red and green.

As a final quality control of inversion results, forward modelling was performed using the 1D V_s average models obtained from surface-wave dispersion inversion. We also used 1D V_s models extracted at each X_{mid} position from the tomography section (see example on Figure 1c). Theoretical dispersion curves calculated from both models were represented over two observed dispersion images extracted along the profile (Figure 2). Dispersion curves computed from surface-wave dispersion inversion results offer a good match with the coherent maxima observed on measured dispersion images. The theoretical fundamental mode is consistent with the picked dispersion curve, and higher modes can be distinguished from each other while they looked like a unique and strong mode at first glance. Interestingly, theoretical dispersion curves calculated from tomography models are clearly following this effective dispersion which remains representative of quick clays since models from both methods are in good agreement in this layer (Figure 1c).

Conclusions

In shallow seismic data, large velocity contrast and/or velocity gradients can generate wavefields with dominant higher modes. Guided waves may also contribute with large amplitudes at high frequencies and phase velocities. In this case, the identification of different propagation modes and the picking of dispersion curves might be challenging and require a thorough analysis of the observed dispersion images, or alternative inversion approaches (Boiero et al. 2013).

The experimental site provided a nice context to address such issues, thanks to its quite simple vertical structure (peat, clays and bedrock) and no strong lateral variations. Tomography methods gave quick and reliable lateral information about seismic velocities. Such low velocity gradient environments however prevent rays from deep propagation, and thus limit the depth of investigation.

Thanks to a careful analysis, surface waves could provide complementary information to refraction tomography results. It should be noted that V_s obtained from both methods are in very good agreement in the quick clay layer. Furthermore, even if tomography failed to depict the peat and the bedrock, it interestingly led to an effective dispersion consistent with an apparent strong unique mode observed on dispersion images.

References

- Bergamo, P., Boiero, D. and Socco, L.V. [2012] Retrieving 2D structures from surface-wave data by means of space-varying spatial windowing. *Geophysics*, **77**(4), EN39-EN51.
- Bodet, L., Abraham, O. and Clorennec, D. [2009] Near-offset effects on Rayleigh-wave dispersion measurements: Physical modeling. *Journal of Applied Geophysics*, **68**(1), 95-103.
- Boiero, D., Wiarda, E. and Vermeer, P. [2013] Surface- and guided-wave inversion for near-surface modeling in land and shallow marine seismic data. *The Leading Edge*, **32**(6), 638-646.
- Forbriger, T. [2003a] Inversion of shallow-seismic wavefields: I. Wavefield transformation. *Geophysical Journal International*, **153**(3), 719-734.
- Forbriger, T. [2003b] Inversion of shallow-seismic wavefields: II. Inferring subsurface properties from wavefield transforms. *Geophysical Journal International*, **153**(3), 735-752.
- Konstantaki, L., Carpentier, S., Garofalo, F., Bergamo, P. and Socco, L.V. [2013] Determining hydrological and soil mechanical parameters from multichannel surface-wave analysis across the Alpine Fault at Inchbonnie, New Zealand. *Near Surface Geophysics*, **11**(4), 435-448.
- O'Neill, A. and Matsuoka, T. [2005] Dominant higher surface-wave modes and possible inversion pitfalls. *Journal of Environmental & Engineering Geophysics*, **10**(2), 185-201.
- Sauvin, G., Lecomte, I., Bazin, S., L'Heureux, J.-S., Vanneste, M., Solberg, I.-L. and Dalsegg, E. [2013] Towards geophysical and geotechnical integration for quick-clay mapping in Norway. *Near Surface Geophysics*, **11**(6), 613-623.
- Schuster, G.T. and Quintus-Bosz, A. [1993] Wavepath eikonal travelttime inversion: Theory. *Geophysics*, **58**(9), 1314-1323.
- Sheehan, J.R., Doll, W.E. and Mandell, W.A. [2005] An evaluation of methods and available software for seismic refraction tomography analysis. *Journal of Environmental & Engineering Geophysics*, **10**(1), 21-34.
- Socco, L.V., Foti, S. and Boiero, D. [2010] Surface-wave analysis for building near-surface velocity models - Established approaches and new perspectives. *Geophysics*, **75**(5), 75A83-75A102.
- Wathelet, M., Jongmans, D. and Ohrnberger, M. [2004] Surface-wave inversion using a direct search algorithm and its application to ambient vibration measurements. *Near Surface Geophysics*, **2**(4), 211-221.